Journal of Molecular Structure 1232 (2021) 130045

Contents lists available at ScienceDirect

Journal of Molecular Structure

journal homepage: www.elsevier.com/locate/molstr

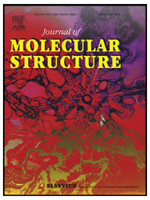

Formation of a potassium coordination polymer based on a novel 2-sulfono-benzene-1,3,5-tricarboxylic acid: Synthesis, characterization, and application of the organocatalyst in CO_2 cycloaddition reaction

Masoumeh Karimi Alavijeh[a], Mostafa M. Amini[a,*], Behrouz Notash[a], Gholamhossein Mohammadnezhad[b,*]

[a] Department of Inorganic Chemistry and Catalysis, Shahid Beheshti University, Tehran, Iran
[b] Department of Chemistry, Isfahan University of Technology, Isfahan 8415683111, Iran

ARTICLE INFO

Article history:
Received 21 October 2020
Revised 19 January 2021
Accepted 30 January 2021
Available online 9 February 2021

Keywords:
Potassium
Coordination polymer
Single-crystal
Carbon dioxide
Cyclic carbonate

ABSTRACT

In the present work, a new 3D potassium coordination polymer (**1**) was prepared by oxidation of sulfonated mesitylene. Its novel sulfono-tricarboxylic ligand, 2-sulfono-benzene-1,3,5-tricarboxylic acid (**2**), which acted as a structure-directing building block, was successfully synthesized by ion exchange of the potassium coordination polymer (**1**). The 3D coordination polymer and the sulfonate-carboxylate ligand were characterized by FT-IR and ^1H and ^{13}C NMR spectroscopies, and their molecular structures were determined by single-crystal X-ray diffraction. In addition, thermal stability and adsorption/desorption behavior of **1** was investigated by TGA-DTA and N_2 adsorption/desorption techniques, respectively. The catalytic activities of the ligand, as a novel and simple organocatalyst, and the rarely explored potassium CPs were studied in the CO_2 cycloaddition reaction. The results showed **2** is an efficient organocatalyst in the CO_2 cycloaddition process. It is suggested that the synergetic effect among Brønsted acid COOH, Lewis base I^- and free water molecules facilitate this reaction.

1. Introduction

Coordination polymers (CPs) are considered superior crystalline materials with widespread applications [1–5]. Different physical and chemical properties of CPs highlight them among other advanced materials. Exceptional high surface area, sorption capacity, acid/base Lewis or Brønsted sites, and facile tunability are some of their important characteristics [6–8]. CPs have intriguing architectures and topologies, which originate mainly from the nature of ligands and metal-centers coordination abilities. Multifunctional organic ligands are vital structure-directing building blocks in CPs and MOFs (metal organic frameworks) [9–14]. Bifunctional sulfonate-carboxylate organic ligands with strong and weak coordination ability of carboxylate and sulfonate functional groups, respectively, have been used in the synthesis of CPs [15–18]. It has also been known that potassium metal salts are efficient catalysts for the synthesis of cyclic carbonates (CCs) from CO_2 [19,20].

In recent years, direct attention has been devoted to CO_2 conversion not only for the adverse effect of CO_2 on global warming and climate change [21] but also as a primer source of C1 [22] for the production of fine chemicals and fuels [23,24]. Besides the scientific and technological improvement, some principle issues remain, such as high energy demand for CO_2 activation [25], difficulties in separation of catalysts from the reaction mixture, and low catalytic activities of heterogeneous catalysts for these processes. Up to now, different methods and systems have been applied to improve this reaction [26]. A suitable method for synthesizing low energy CCs is the cycloaddition of CO_2 to diverse, high-energy epoxides [27]. CCs are considered as an important class of compounds in chemical industries. Various types of metal-based homogeneous and heterogeneous catalysts can catalyze this reaction including metal salts [27,28], metal oxides [29–31], oxychlorides [32], porphyrin [33], phthalocyanine [34], and salen complexes [32,35–37], immobilized nanoparticles [38], highly ordered microporous and mesoporous materials [39,40], and more recently coordination polymers (CPs) and MOFs [41–45]. An alternative that has been proved to be more efficient in milder conditions (lower pressure and temperature) is organocatalysts [46].

In this work, a new 3D potassium coordination polymer with intriguing structural aspects and a novel bifunctional sulfonate-carboxylate organic ligand, 2-sulfono-benzene-1,3,5-tricarboxylic acid ($H_3BTC-SO_3.H_3O$), were successfully synthesized and charac-

---

[*] Corresponding authors.
E-mail addresses: m-pourmini@sbu.ac.ir (M.M. Amini), mohammadnezhad@iut.ac.ir (G. Mohammadnezhad).

https://doi.org/10.1016/j.molstruc.2021.130045
0022-2860/

terized. $H_3BTC\text{-}SO_3^-$ acted as a structure-directing building block in the synthesized potassium CP. The catalytic activities of the $H_3BTC\text{-}SO_3.H_3O$, as a novel, simple organocatalyst, and the rarely explored potassium CPs were studied in the CO_2 cycloaddition reaction.

2. Experimental

2.1. Materials and instrumentation

All chemicals and solvents were commercially available and used without purification. Infrared spectra were recorded on a Bomem MB-Series FTIR spectrometer. ^1H and ^{13}C NMR data were collected on a Bruker AVANCE 300 MHz spectrometer utilizing D_2O as solvent and tetramethylsilane as an internal standard. A STOE diffractometer equipped with Cu K_α radiation ($\lambda = 0.15418$ nm) was used to record powder X-ray diffraction (XRD) patterns. Thermogravimetric analysis (TGA) was performed using a Bahr STA-503 instrument at a heating rate of 10 °C min^{-1} under airflow. The CHN elemental analysis was accomplished using a Perkin-Elmer 2400 CHN analyzer.

2.1.1. X-ray crystallography

The X-ray diffraction measurements were made on a STOE IPDS-II diffractometer with graphite-monochromated Mo-$K\alpha$ radiation. Single-crystals of **1** and **2** were mounted on glass fiber and used for data collection. Cell constants and an orientation matrix for data collection were obtained by the least-square refinement of 7248, 7588 reflections for **1** and **2**, respectively. Both data were collected at room temperature to a maximum 2θ value of 58.32 and 58.34° for **1** and **2**, respectively. Diffraction data were collected in a series of ω scans in 1° oscillation and integrated using the Stoe X-AREA [47] software package. Numerical absorption correction was applied using X-RED [48] and X-SHAPE [49] software. The data were corrected for Lorentz and polarizing effects. The structures were solved by direct methods [50] and subsequent difference Fourier maps and then refined on F^2 by a full-matrix least-squares procedure using anisotropic displacement parameters [51]. Atomic factors are from the International Tables for X-ray Crystallography [52]. All refinements were performed using the X-STEP32 crystallographic software package [53]. In compound **2**, all hydrogens attached to oxygens were found in a difference Fourier maps and refined isotropically. Other hydrogen atoms were positioned geometrically and refined as riding atoms with $C—H = 0.93$ Å, Uiso(H) = 1.2Ueq(C). Crystal data and refinement for compounds **1** and **2** are summarized in Table S1, and selected bond length and angles are given in Table S2 and Table S3 in the ESI†.

2.2. Synthesis of $[K(H_3BTC\text{-}SO_3)(H_2O)_2]_n$ (1) and $(C_9H_5O_9S).H_3O\cdot 2H_2O$ ($(H_3BTC\text{-}SO_3).H_3O\cdot 2H_2O$) (2)

For the synthesize of **1**, 5 mL of mesitylene was poured into a round bottom flask, then 4 mL of the oleum was added, and the mixture was stirred for 5 min. The resulting white precipitate was filtered and dried at ambient temperature. Subsequently, the sulfonated mesitylene (10.42 g, 0.056 mol) was dissolved in 250 mL of deionized water in a 500 mL round bottom flask. The flask was placed in the ice bath, and then $KMnO_4$ (41.18 g, 0.26 mol) was added stepwise in 3 h. Then, the reaction mixture was refluxed for 48 h and then filtered to remove the residual MnO_2. After the addition of HCl to the filtrate, the solution allowed to crystallize by slow evaporation. The resulting colorless crystals were collected and characterized by FTIR, ^1H-, and ^{13}C NMR spectroscopies and CHN analysis. The structure of the complex was determined by single-crystal X-ray diffraction. Anal. Calcd. (Found) for $C_9H_9KO_{11}S$: C 29.67 (29.09); H 2.49 (2.38). ^1H NMR (300 MHz, D_2O) δ (ppm): 8.08 (s, 2H, 2 (Ar—H)). ^{13}C NMR (75.43 MHz, D_2O): δ (ppm): 171.5, 167.4 ($C = O$), 140.9, 134.0, 132.7, 130.0 (Ar). IR bands (KBr) ῡ (cm^{-1}) 523, 630, 651, 700, 758, 845, 907, 1019, 1081, 1188, 1245, 1306, 1414, 1608, 1726, 3032, 3083, 3288, 3510, and 3595.

For the preparation of $(H_3BTC\text{-}SO_3).H_3O\cdot 2H_2O$ (BTC = 1,3,5-benzenetricarboxylate) (**2**), 250 mg of **1** was dissolved in 20 mL of deionized water and pass through a column (20 × 1 cm) containing Dowex-50W-X8, a strongly acidic cation-exchange resin. The column was eluted by deionized water, and the resulted solution was collected and allowed to crystalize by slow evaporation of water at room temperature. The titled compound was characterized by FTIR, ^1H-, and ^{13}C NMR spectroscopies, and the structure of **2** was determined by single-crystal X-ray diffraction. Anal. Calcd. (Found) for $C_9H_{12}O_{12}S$: C 31.40 (31.22); H 3.51 (3.65). ^1H NMR (300 MHz, D_2O) δ (ppm): 8.10 (s, 2H, 2 (Ar—H)). ^{13}C NMR (75.43 MHz, D_2O): 171.3, 167.4 ($C = O$), 141.0, 133.8, 132.3, 130.1 (Ar). IR bands (KBr) ῡ (cm^{-1}): 518, 625, 661, 701, 758, 860, 912, 1020, 1076, 1194, 1245, 1322, 1409, 1614, 1731, 3030, 3077, and 3430.

2.3. Cycloaddition reaction of CO_2 with epoxide and catalyst regeneration

In a typical procedure, 4 mmol styrene oxide, 5 mol% TBAB (tetrabutylammonium bromide) and 5 mol% catalyst were loaded into a vial, which was filled with 1 atm of CO_2. The reaction mixture was stirred at 110 °C for 10 h, and after cooling, some chloroform was added to the reaction vessel, and the catalyst was removed by centrifugation. Purification of the crude product was performed by column chromatography using ethyl acetate/n-hexane (1:3, v:v) as an eluent to obtain the pure product. mp 49–51 °C (lit. 50–51 °C) [54,55]. ^1H NMR (300 MHz, $CDCl_3$) δ (ppm): 4.40 (t, 1H, ($-CH_2$)), 4.84 (t, 1H, ($-CH_2$)), 5.70 (t, 1H, ($-CH$)), 7.37–7.49 (m, 5H, Ph). After each catalytic cycle, the catalyst was separated by centrifugation from the reaction mixture, washed with chloroform, and dried at 80 °C for the next catalytic run.

3. Results and discussion

3.1. Synthesis of the compounds

Bifunctional-substituted isomers of tricarboxylate monosulfate aromatic compounds have rarely been explored. Three different structures of monosulfono-benzene-tricarboxylic acid have been found in literature, as shown in Scheme 1. Metal salts of 5-sulfono-benzene-1,3,5-tricarboxylic acid (5-sulfonyl-1,2,4-benzenetricarboxylic acid or 1,2,4C-5S) are commercially available. They have been used to synthesize different CPs and MOFs [56,57], while the structures of the other two have been found in two patents with no further information [58]. In this study 2-sulfono-benzene-1,3,5-tricarboxylic acid (1,3,5–2S or $H_3BTC\text{-}SO_3.H_3O$), were successfully synthesized in two-step, as shown in Scheme 2. Sulfonation of mesitylene has been performed in the first step. It should be mentioned that the synthesis of sulfonated mesitylene has previously been reported by other methods [59,60], in the presence of different catalysts at a higher temperature and longer time with a lower yield. Sulfonated mesitylene in this work was prepared in much higher yield using oleum at ambient temperature only in 5 min. In the next step, the methyl groups were successfully oxidized, and after work up a potassium CP and the first coordination polymer of the $H_3BTC\text{-}SO_3$ has been formed. The pure crystalline ligand $(H_3BTC\text{-}SO_3).H_3O\cdot 2H_2O$ (**2**) was obtained by the ion-exchange technique.

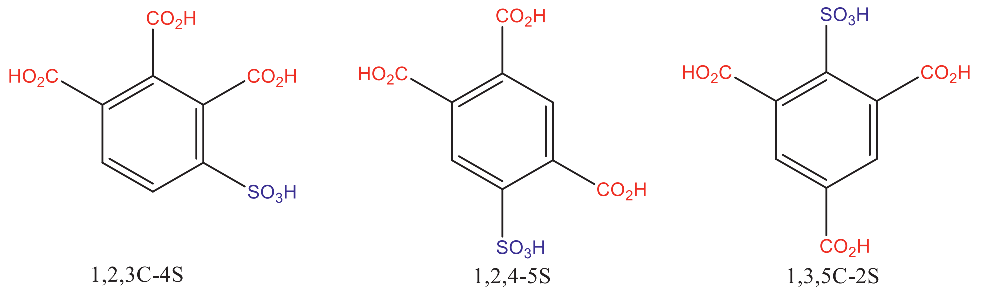

Scheme 1. Three different structures of monosulfono-benzene-tricarboxylic acids.

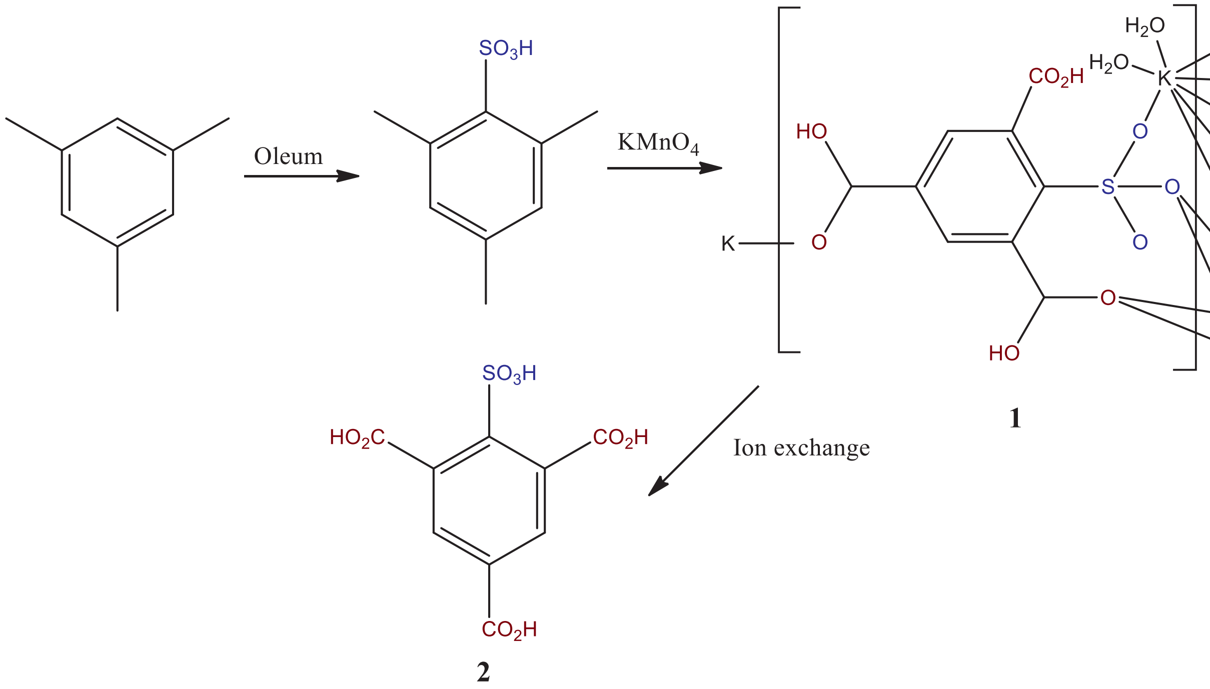

Scheme 2. The synthetic procedure of $[K(H_3BTC\text{-}SO_3)(H_2O)_2]_n$ (**1**) and $(H_3BTC\text{-}SO_3).H_3O\cdot 2H_2O$ (**2**).

3.2. Crystal structure of $[K(H_3BTC\text{-}SO_3)(H_2O)_2]_n$) (1) and ($(H_3BTC\text{-}SO_3).H_3O\cdot 2H_2O$) (2)

Compound **1** is a potassium coordination polymer that is constructed of a neutral $[K(H_3BTC\text{-}SO_3)(H_2O)_2]$ complex. The asymmetric unit of **1** consists of a K^+ ion, a $H_3BTC\text{-}SO_3^-$ ligand, and two water molecules (O10 and O11), as shown in Fig. 1. The coordination number of potassium ion, K1, is eight and form a distorted square-antiprism by three oxygens of sulfonate groups: O6, O6, and O7, three oxygens of carboxylate groups: O2, O9 and O9, and two oxygens from water molecules: O10 and O11. The bond lengths of K1—O range from 2.761(3) to 3.0642(18) Å (see Table S2) and are consistent with reported values in the literature [61]. Two sulfonate oxygens and two oxygens of carboxylate groups are in bridging position and resulted in a four and six-member cage-like 2D inorganic layer (Fig. 2). These 2D layers are connected by the organic pillars, $H_3BTC\text{-}SO^{3-}$ ligand, *via* O2 and O9 atoms of carboxylate groups and O7 atom of sulfonate groups to generate a 3D framework (Fig. 3). Interestingly, one of the carboxylate groups are left free and have the potential for further reactions.

Compound **2** was crystallized in the triclinic crystal system and $P\bar{1}$ space group with two formula units in the unit cell ($Z = 2$). The asymmetric unit of **2** is shown in Fig. 4, which consists of $H_3BTC\text{-}SO_3^-$, H_3O^+, and two water molecules. The two C–O bonds lengths in each of the carboxylate groups are not identical, ca. 1.2 *vs.* 1.3 Å, which is an indication of the protonated oxygen atoms. All of the hydrogens except the two phenyl ring hydrogens are participate in extended three-dimensional hydrogen bonding. For instance, one of the two independent H_2O molecules (O9) formed a dimer *via* both of its hydrogens, as shown in Fig. 5. A variety of H-bondings were present in **2** and formed a 3D network.

3.3. FT-IR spectra, PWXRD patterns, and thermogravimetric analyses

Fig. 6 shows the FT-IR spectra of sulfonated mesitylene, compounds **1** and **2**. The bands observed at 3510 and 3595 cm^{-1} in the FT-IR spectrum of compound **1** (Fig. 6b) demonstrated the presence of coordinated water molecules in the titled compound [62]. The emergence of the new bands at 1245, 1306, and 1726 cm^{-1} attributed to the stretching vibrations of C–O and $C = O$ bonds of the carboxylic acid [62]. The disappearance of the C–H stretching bands at 2850 and 2930 cm^{-1} in the spectrum of sulfonated mesitylene (Fig. 6a) indicates methyl groups oxidation to carboxylic acid functional groups. Apparently, after passing the potassium coordination polymer through the ion exchange column, coordinated water molecules were eliminated, and 2-sulfono-benzene-1,3,5-tricarboxylic acid formed. Also, the bands at 661, 1020, 1076, and 1194 cm^{-1} in the spectrum of compounds **2** (Fig. 7c) associated with the stretching vibration of C–S, the stretching vibration of $S - O$, the in-plane skeletal vibration of the benzene ring with a

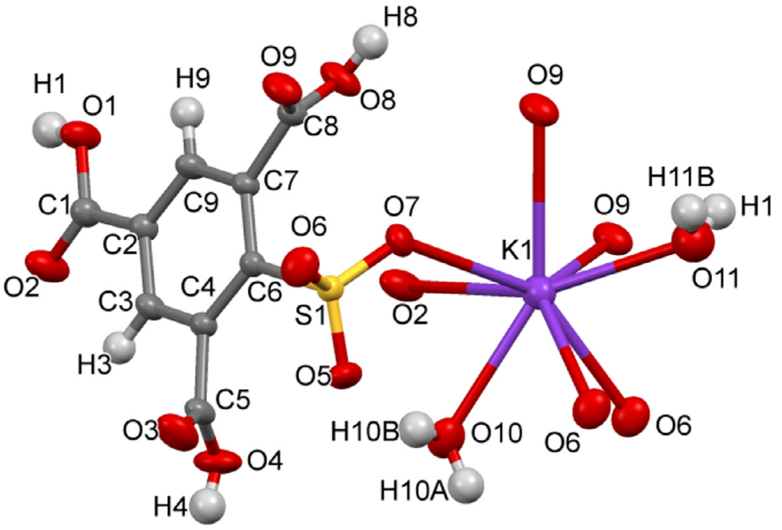

Fig. 1. Crystal structure of **1** showing potassium ion surroundings with 50% of probability.

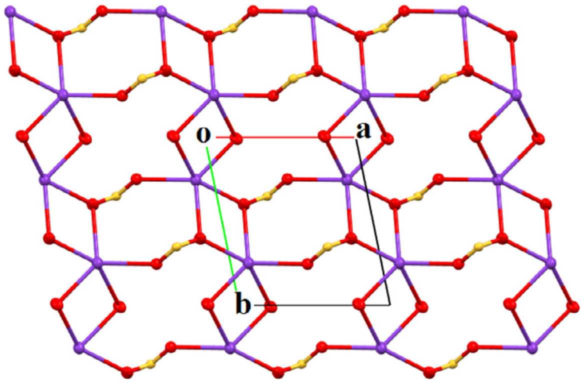

Fig. 2. Representation of 2D inorganic layer of **1** along *c* axis. The bridging oxygens, potassium, and sulfur are only shown for more clarity.

sulfonic substituent, and the symmetric stretching vibration mode of $O = S = O$, respectively [63–65].

The X-ray powder diffraction of compound **1**, and its simulated pattern, are presented in Fig. 7. Both of the patterns are closely matched, which implies the purity and crystallinity of the bulk material of compound **1**. Also, the XRD pattern of compound **2** approved the crystallinity of the bulk material, see Figure S1.

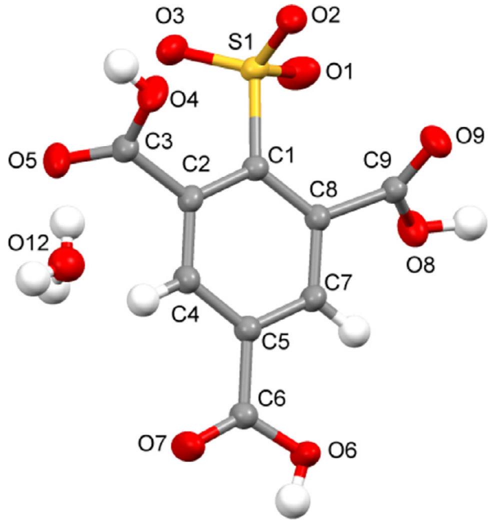

Fig. 4. The asymmetric unit of **2** (water molecules are not shown for more clarity). The ellipsoids are drawn with 50% probability. Hydrogen atoms are presented with ball and stick style.

TGA and DTA curves of compound **1** are shown in Fig. 8. The 5 wt.% mass loss at about 165 °C in the TGA curve, which

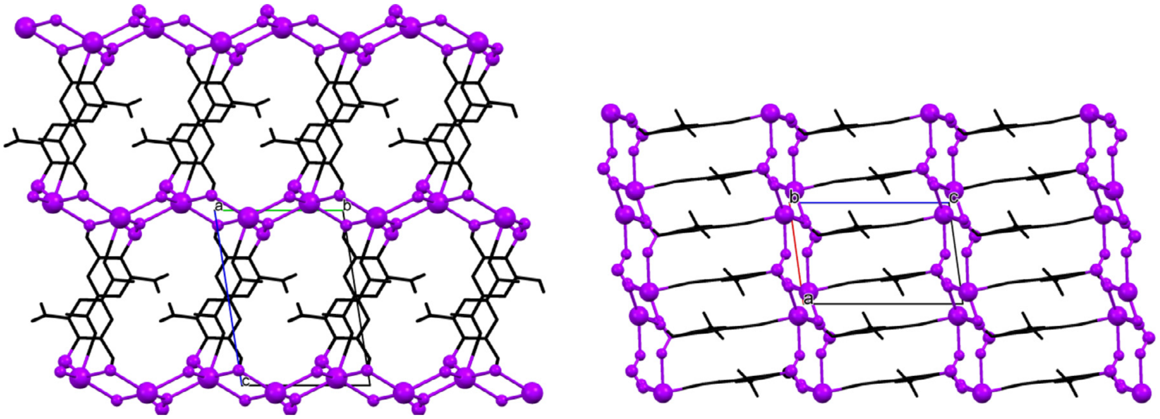

Fig. 3. Representation of 3D framework of **1** along *a* and *b* axis. The 2D inorganic layers are presented in purple color, and organic pillars are shown in black color. (For interpretation of the references to colour in this figure legend, the reader is referred to the web version of this article.)

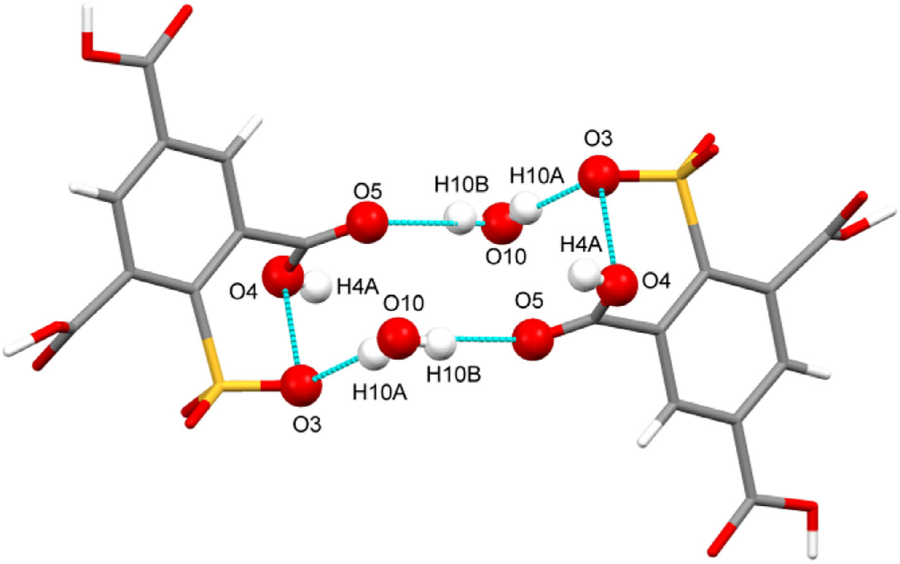

Fig. 5. Hydrogen bonds formation *via* H_2O, carboxylate, and sulfonate.

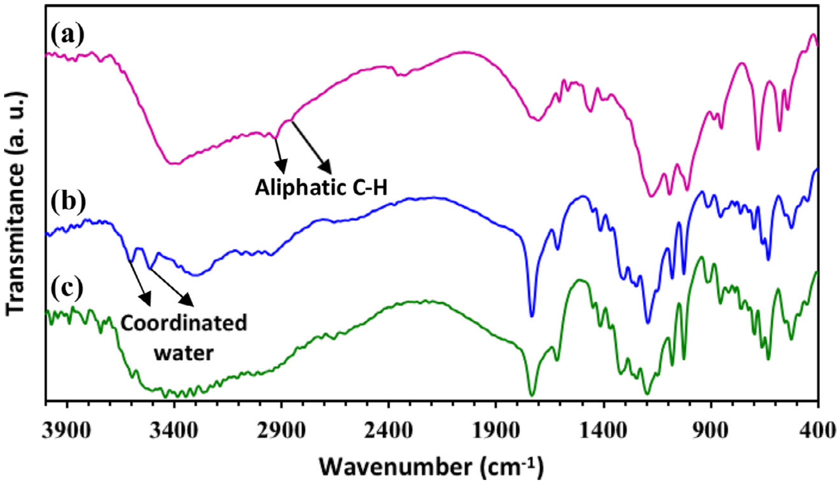

Fig. 6. FT-IR spectra of the sulfonated mesitylene (a), compound **1** (b), and compound **2** (c).

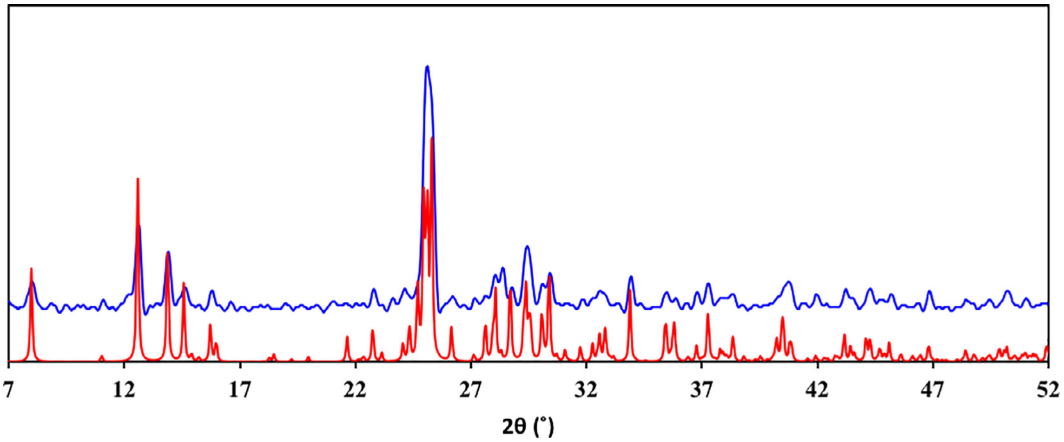

Fig. 7. Simulated XRD patterns of compound **1** based on the single-crystal structure (down, red), and its experimental pattern (top, blue).

is accompanied by an endothermic peak in the DTA curve, is associated with the dehydration and release of two coordinated water molecules in the complex. The second endothermic step in the temperature range of 250–310 °C in the DTA curve and almost without mass loss in the TGA curve can be attributed to the decomposition and collapse of coordination polymer structure. Finally, the substantial mass loss that occurs from 310–800 °C in the TGA curve along with the several exothermic peaks in the DTA curve is due to the combustion of decomposition products, organic residue, and the possible trace of charcoal, which extend combustion to around of 800 °C.

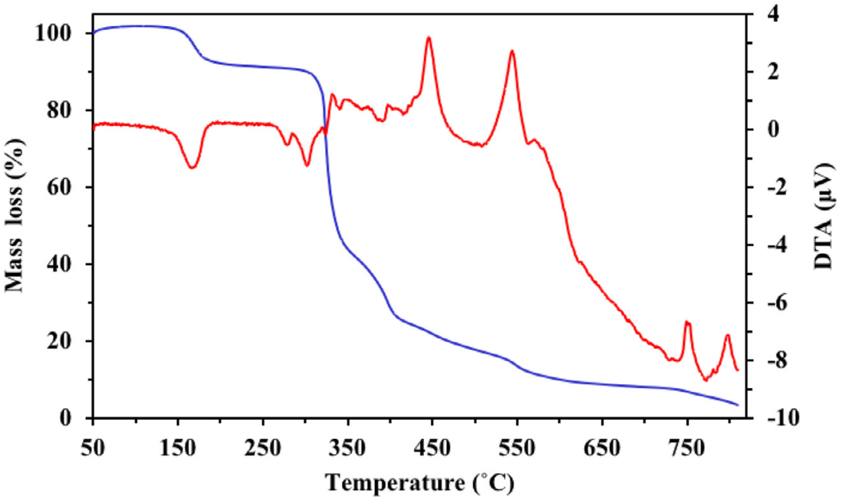

Fig. 8. Thermogravimetric analysis of the structure **1**.

Table 1
The role of effective factors on the cycloaddition reaction of CO_2 with styrene oxide in the presence of $[K(H_3BTC\text{-}SO_3)(H_2O)_2]_n$ (**1**) and $(H_3BTC\text{-}SO_3).H_3O{\cdot}2H_2O$ (**2**) under atmospheric pressure of carbon dioxide.

Entry	Catalyst (% mol)	Cocatalyst (% mol)	Solvent	T (°C)	t (h)	Yield (%)
1	-	TBAI (5)	neat	110	10	-
2	1 (5)	TBAI (5)	neat	110	10	17
3	2 (5)	TBAB (5)	neat	110	10	40
4	2 (5)	TBAI (5)	neat	110	10	50
5	2 (5)	TBAI (5)	H_2O	110	10	10
6	2 (5)	TBAI (5)	CH_3CN	110	10	-
7	2 (5)	TBAI (5)	CH_3CN	110	10	5
8	2 (5)	TBAI (5)	neat	130	10	52
9	2 (5)	TBAI (5)	neat	90	10	35
10	2 (5)	TBAI (5)	neat	110	14	55
11	2 (5)	TBAI (5)	neat	110	8	40
12	2 (5)	TBAI (5)	neat	110	6	26
13	2 (5)	TBAI (5)	neat	110	10	32
14	2 (8)	TBAI (5)	neat	110	10	53
15	2 (5)	TBAI (2)	neat	110	10	30
16	2 (5)	TBAI (8)	neat	110	10	51
17	2 (5)	TBAI (5)	neat	110	10	81[b]

[a] Isolated yield. [b] CO_2 pressure = 5 bar.

3.4. Catalytic study

The reaction of styrene oxide and CO_2 has been selected as a model reaction for a heterogeneous solvent-free reaction to determine the efficiency of potassium coordination polymer (PCP, **1**) and the linker derived from it (**2**). At the reaction conditions, no product was produced in the absence of the catalyst (Table 1, entry 1). Tetrabutylammonium bromide (TBAB) and tetrabutylammonium iodide (TBAI) were used at different molar percentages with respect to the substrate to determine the effect of cocatalyst on the reaction process of styrene carbonate production from styrene oxide under atmospheric pressure of carbon dioxide. As can be seen, TBAI has a better performance than TBAB, and with increasing molar percentage of TBAI, the reaction efficiency is enhanced, and after reaching the plateau, increasing the amount of cocatalyst has no effect on the reaction process (Table 1, entries 2–3 and 15–16). The differences between cocatalysts arise due to the differences in the donor strength of the Lewis-bases, as mentioned above. As shown in Table 1, entries 2–3, TBAI is the best base for this reaction. By making a simple comparison to TBAB, the iodide provided a much better nucleophilicity resulted in more convenient ring-opening and –closure steps. Also, various studies have shown that this reaction does not progress significantly in the presence of solvents such as water and acetonitrile (Table 1, entries 5–6), which can dissolve **2** as a catalyst. In fact, by dissolving the **2** in the solvent, the structure breaks down and loses its desired spatial position to form the hydrogen bond with the epoxy ring and perform the reaction. The reaction in chloroform as a solvent in which **2** is not soluble also did not yield the desired result (Table 1, entry 7), possibly due to the decrease in the number of effective collisions between the reactants as a result of the lowering concentration. By changing various factors such as temperature, time, and amount of catalyst, the role of these factors in advancing CO_2 fixation reaction was investigated (Table 1, entries 8–14). The results showed that by increasing each of these factors, the production efficiency of styrene carbonate increased. After reaching the plateau, further increasing each item did not cause a noticeable change in the desired product yield.

Based on the catalytic test results, the optimum reaction conditions were selected, and the cycloaddition reaction of CO_2 with styrene oxide reached a maximum efficiency of 81% under 5 bar pressure of carbon dioxide in 10 h at 110 °C in the presence of

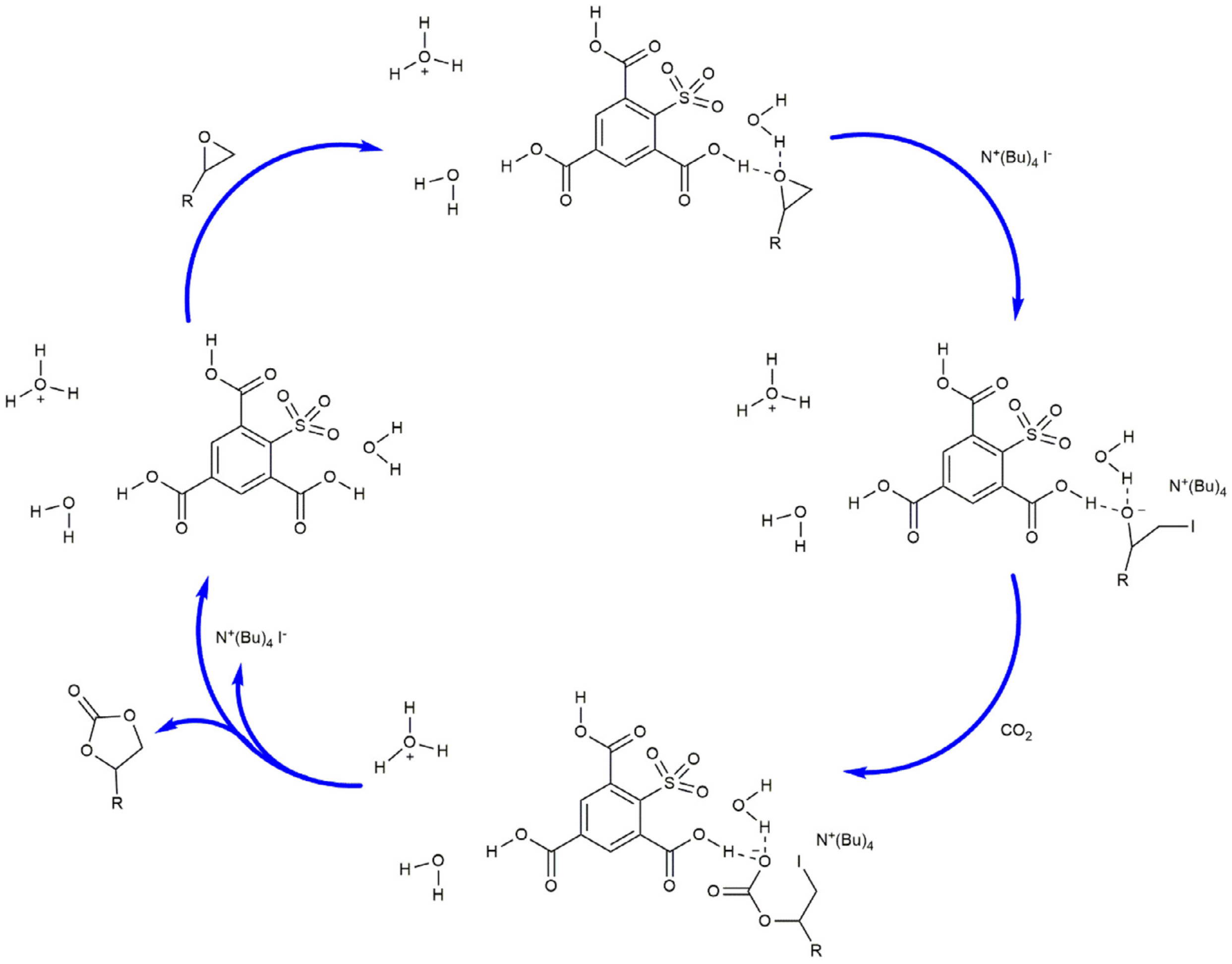

Fig. 9. The plausible mechanism pathway for the cycloaddition reaction of styrene oxide and CO_2 using 2-sulfono-benzene-1,3,5-tricarboxylic acid (**2**).

tetrabutylammonium iodide as a cocatalyst. Furthermore, the catalysts TOF values was lower than 2 h^{-1}.

The catalytic performance of organocatalyst (**2**) was better than PCP (**1)** in the reaction of styrene carbonate synthesis under the same conditions (Table 1, entries 2 and 4). It is interesting to compare **2** and **1** as a catalyst in the cycloaddition reactions and explain the possible reason for the yield differences. It has been found that in the reaction of styrene dioxide and carbon dioxide, hydrogen bond formation plays a vital role in accelerating the reaction [66]. According to the presented mechanism in Fig. 9, the adjacent hydroxyl groups significantly impact the formation of the desired product by forming a hydrogen bond with epoxy ring oxygen and formation the stable 7-membered ring species [67]. Besides, in **1,** because of the spatial congestion around coordinated water molecules to potassium, the possibility of forming a hydrogen bond with the epoxy ring oxygen is reduced compared to **2**. Therefore, the poor performance of **1** compared to **2** (17% vs. 50%) during the cycloaddition reaction is reasonable.

The reusability of the 2-sulfono-benzene-1,3,5-tricarboxylic acid (**2**) as a catalyst in the CO_2 cycloaddition reaction was also evaluated, and it was found to be robust and stable during recovery cycles (Fig. 10).

Table 2 provides a brief comparison of the optimum catalyst performance in this study with previously reported catalysts with a similar mechanism. As can be seen, compared to similar catalysts reported in the literature, 2-sulfono-benzene-1,3,5-tricarboxylic acid (**2**) has advantages such as fast, convenience, and reasonable yield in the low pressure of CO_2.

Table 2
Comparison of the catalytic performance of 2-sulfono-benzene-1,3,5-tricarboxylic acid (**2**) with previously reported catalysts in neat condition.

Entry	Catalyst	T (°C)	t (h)	CO_2 pressure (bar)	Yield (%)	Ref.
1	$NaI/PPh_3/PhOH$	120	14	40	100	[68]
2	Cellulose/KI	110	9	20	98	[69]
3	Potassium complex	150	8	22	50	[70]
4	EDTA	70	18	5	94	[43]
5	$[\{(CH_2)_3CO_2H\}im]Br$	120	1	20	95	[71]
6	PDVB-CEIMBr	140	4	20	93.8	[72]
7	$\{[Zn_2(H_2L)_2](NO_3)_4\}_n$ (CP-1)	100	4	10	99	[73]
8	Cobalt-based CP	80	2	10	59	[74]
9	**2**	110	10	5	81	This work

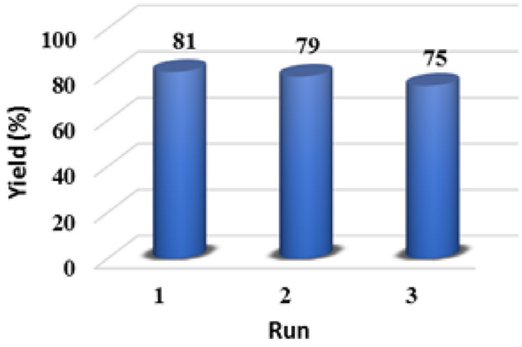

Fig. 10. The reusability of **2** in the preparation of styrene carbonate from styrene oxide under CO_2 pressure 5 bar.

4. Conclusion

In this study, two new compounds, potassium coordination polymer, and the corresponding ligand, were introduced and they used to investigate their performance as catalysts in the cycloaddition of CO_2 to epoxides. The results showed that the ligand of potassium coordination polymer, carboxylic acid-containing ligand, as a heterogeneous organocatalyst had a better performance than potassium coordination polymer under the same reaction conditions. The remarkable performance of ligand in the cycloaddition of CO_2 to epoxides confirmed the synergistic effects of the simultaneous presence of Brønsted acid COOH, Lewis base I^- and free water molecules during the reaction. This organocatalyst can be reused and recovered without significant loss in efficiency over several consecutive steps.

Declaration of Competing Interest

The authors declare that they have no known competing financial interests or personal relationships that could have appeared to influence the work reported in this paper.

CRediT authorship contribution statement

Masoumeh Karimi Alavijeh: Investigation, Software, Writing – original draft. **Mostafa M. Amini:** Project administration, Supervision, Funding acquisition, Conceptualization, Writing – review & editing. **Behrouz Notash:** Formal analysis, Methodology. **Gholamhossein Mohammadnezhad:** Visualization, Writing – review & editing, Data curtion, Software.

Acknowledgements

Authors gratefully acknowledge the research consular of Shahid Beheshti University and the Isfahan University of Technology for financial support.

References

[1] A.H. Chughtai, N. Ahmad, H.A. Younus, A. Laypkov, F. Verpoort, Metal–organic frameworks: versatile heterogeneous catalysts for efficient catalytic organic transformations, Chem. Soc. Rev. 44 (2015) 6804–6849.
[2] J.-.R. Li, Y. Ma, M.C. McCarthy, J. Sculley, J. Yu, H.-.K. Jeong, P.B. Balbuena, H.-.C. Zhou, Carbon dioxide capture-related gas adsorption and separation in metal-organic frameworks, Coord. Chem. Rev. 255 (2011) 1791–1823.
[3] T. Zhang, W. Lin, Metal–organic frameworks for artificial photosynthesis and photocatalysis, Chem. Soc. Rev. 43 (2014) 5982–5993.
[4] H. Deng, S. Grunder, K.E. Cordova, C. Valente, H. Furukawa, M. Hmadeh, F. Gándara, A.C. Whalley, Z. Liu, S. Asahina, Large-pore apertures in a series of metal-organic frameworks, Science 336 (2012) 1018–1023.
[5] J.-.P. Zhang, Y.-.B. Zhang, J.-.B. Lin, X.-.M. Chen, Metal azolate frameworks: from crystal engineering to functional materials, Chem. Rev. 112 (2012) 1001–1033.
[6] A. Corma, H. García, F. Llabrés i Xamena, Engineering metal organic frameworks for heterogeneous catalysis, Chem. Rev. 110 (2010) 4606–4655.
[7] J. Liu, L. Chen, H. Cui, J. Zhang, L. Zhang, C.-.Y. Su, Applications of metal-organic frameworks in heterogeneous supramolecular catalysis, Chem. Soc. Rev. 43 (2014) 6011–6061.
[8] Z. Zhou, C. He, J. Xiu, L. Yang, C. Duan, Metal–organic polymers containing discrete single-walled nanotube as a heterogeneous catalyst for the cycloaddition of carbon dioxide to epoxides, J. Am. Chem. Soc. 137 (2015) 15066–15069.
[9] K.-.J. Chen, R.-.B. Lin, P.-.Q. Liao, C.-.T. He, J.-.B. Lin, W. Xue, Y.-.B. Zhang, J.-.P. Zhang, X.-.M. Chen, New Zn-aminotriazolate-dicarboxylate frameworks: synthesis, structures, and adsorption properties, Cryst. Growth Des. 13 (2013) 2118–2123.
[10] G.K. Shimizu, R. Vaidhyanathan, J.M. Taylor, Phosphonate and sulfonate metal organic frameworks, Chem. Soc. Rev. 38 (2009) 1430–1449.
[11] A. Mietrach, T.W. Muesmann, J. Christoffers, M.S. Wickleder, Sulfonic Acid Analogs of Terephthalic and Trimesic Acid as Linkers in Metal-organic frameworks–synthesis of thermally robust MOFs, Eur. J. Inorg. Chem. 2009 (2009) 5328–5334.
[12] A. Mietrach, T.W. Muesmann, C. Zilinski, J. Christoffers, M.S. Wickleder, Benzene Trisulfonic Acid (H_3BTS) as Analogue of Trimesic Acid for Building Open Frameworks: the First Rare Earth Examples $[La(BTS)(H_2O)_5]$ and $[RE(BTS)(H_2O)_4]$ (RE= Nd, Sm, Eu), Z. Anorg. Allg. Chem. 637 (2011) 195–200.
[13] T.W. Muesmann, C. Zitzer, A. Mietrach, T. Klüner, J. Christoffers, M.S. Wickleder, para-Benzene disulfonic acid and its tetrachloro and tetrafluoro derivatives—Studies towards polyhalogenated metal–organic-frameworks with sulfo analogues of terephthalic acid, Dalton Trans. 40 (2011) 3128–3141.
[14] T.W. Muesmann, A. Mietrach, J. Christoffers, M.S. Wickleder, Synthesis of 1,2,4,5-benzenetetrasulfonic acid (H_4B_4S) and its implementation as a linker for building metal-organic frameworks on the example of $[Cu_2(B_4S)(H_2O)_8]\cdot 0{\cdot}5H_2O$, Z. Anorg. Allg. Chem. 636 (2010) 1307–1312.
[15] A.D. Kulynych, G.K. Shimizu, A pseudo-honeycomb coordination net formed with 5-sulfoisophthalic acid, Cryst. Eng. Comm. 4 (2002) 102–105.
[16] X.-.H. Miao, L.-.G. Zhu, Synthesis, supramolecular structures and catalytic properties of nickel(II) 3-sulfobenzoate complexes with chelating amine ligands, Cryst. Eng. Comm. 11 (2009) 2500–2509.
[17] G. Prochniak, V. Videnova-Adrabinska, M. Daszkiewicz, A. Pietraszko, packing patterns and network entanglements in sodium and silver(I) 3-carboxybenzenesulfonate crystals, J. Mol. Struct. 891 (2008) 178–183.
[18] I. Papadaki, C.D. Malliakas, T. Bakas, P.N. Trikalitis, Molecular supertetrahedron decorated with exposed sulfonate groups built from mixed-valence tetranuclear $Fe_3{}^{3+}Fe^{2+}(\mu_3\text{-}O)(\mu_3\text{-}SO_4)_3(-CO_2)_3$ clusters, Inorg. Chem. 48 (2009) 9968–9970.
[19] T. Werner, N. Tenhumberg, Synthesis of cyclic carbonates from epoxides and CO_2 catalyzed by potassium iodide and amino alcohols, J. CO_2 Util. 7 (2014) 39–45.
[20] J.W. Comerford, I.D. Ingram, M. North, X. Wu, Sustainable metal-based catalysts for the synthesis of cyclic carbonates containing five-membered rings, Green Chem. 17 (2015) 1966–1987.
[21] G. Peters, R. Andrew, J. Canadell, P. Friedlingstein, R. Jackson, J. Korsbakken, C.Le Quéré, A. Peregon, Carbon dioxide emissions continue to grow amidst slowly emerging climate policies, Nat. Clim. Chang 10 (2020) 3–6.
[22] Z. Zhang, S.-.Y. Pan, H. Li, J. Cai, A.G. Olabi, E.J. Anthony, V. Manovic, Recent advances in carbon dioxide utilization, Renew. Sustain. Energy Rev. 125 (2020) 109799.
[23] J. Artz, T.E. Müller, K. Thenert, J. Kleinekorte, R. Meys, A. Sternberg, A. Bardow, W. Leitner, Sustainable conversion of carbon dioxide: an integrated review of catalysis and life cycle assessment, Chem. Rev. 118 (2018) 434–504.
[24] a) S.S. Dhankhar, B. Ugale, C.M. Nagaraja, Co-catalyst-free chemical fixation of CO_2 into cyclic carbonates by using metal-organic frameworks as efficient heterogeneous catalysts, Chem.: Asian J 15 (2020) 2403–2427; b) A. Hosseinian, S. Farshbaf, R. Mohammadi, A. Monfared, E. Vessally, Advancements in six-membered cyclic carbonate (1,3-dioxan-2-one) synthesis utilizing carbon dioxide as a C1 source, RSC adv 8 (2018) 17976–17988; c) H. Büttner, L. Longwitz, J. Steinbauer, C. Wulf, T. Werner, Recent developments in the synthesis of cyclic carbonates from epoxides and CO_2, Topics Curr. Chem. 375 (2017) 1–56.
[25] C. Song, Global challenges and strategies for control, conversion and utilization of CO_2 for sustainable development involving energy, catalysis, adsorption and chemical processing, Catal. Today 115 (2006) 2–32.
[26] T. Sakakura, J.-.C. Choi, H. Yasuda, Transformation of carbon dioxide, Chem. Rev. 107 (2007) 2365–2387.
[27] H. Jing, S.T. Nguyen, $SnCl_4$-organic base: highly efficient catalyst system for coupling reaction of CO_2 and epoxides, J. Mol. Catal. A 261 (2007) 12–15.
[28] Z. Xi, Y. Zhang, Y. Xiangui, Y. Jie, W. Gongying, Hydrated alkali metal halides as efficient catalysts for the synthesis of cyclic carbonates from CO_2 and epoxides, Chin. J. Catal. 31 (2010) 765–768.
[29] K. Yamaguchi, K. Ebitani, T. Yoshida, H. Yoshida, K. Kaneda, Mg—Al mixed oxides as highly active acid—base catalysts for cycloaddition of carbon dioxide to epoxides, J. Am. Chem. Soc. 121 (1999) 4526–4527.
[30] M. Aresta, A. Dibenedetto, L. Gianfrate, C. Pastore, Nb(V) compounds as epoxides carboxylation catalysts: the role of the solvent, J. Mol. Catal. A 204 (2003) 245–252.
[31] W.-.L. Dai, S.-.F. Yin, R. Guo, S.-.L. Luo, X. Du, C.-.T. Au, Synthesis of propylene carbonate from carbon dioxide and propylene oxide using Zn-Mg-Al composite oxide as high-efficiency catalyst, Catal. Lett. 136 (2010) 35–44.

[32] H. Yasuda, L.-N. He, T. Sakakura, Cyclic carbonate synthesis from supercritical carbon dioxide and epoxide over lanthanide oxychloride, J. Catal. 209 (2002) 547–550.

[33] R.L. Paddock, Y. Hiyama, J.M. McKay, S.T. Nguyen, Co(III) porphyrin/DMAP: an efficient catalyst system for the synthesis of cyclic carbonates from CO_2 and epoxides, Tetrahedron Lett. 45 (2004) 2023–2026.

[34] D. Ji, X. Lu, R. He, Syntheses of cyclic carbonates from carbon dioxide and epoxides with metal phthalocyanines as catalyst, Appl. Catal. A 203 (2000) 329–333.

[35] D.J. Darensbourg, Making plastics from carbon dioxide: salen metal complexes as catalysts for the production of polycarbonates from epoxides and CO_2, Chem. Rev. 107 (2007) 2388–2410.

[36] J. Melèndez, M. North, R. Pasquale, Synthesis of cyclic carbonates from atmospheric pressure carbon dioxide using exceptionally active aluminium (salen) complexes as catalysts, Eur. J. Inorg. Chem. 2007 (2007) 3323–3326.

[37] E.K. Noh, S.J. Na, S.-W. Kim, B.Y. Lee, Two components in a molecule: highly efficient and thermally robust catalytic system for CO_2/epoxide copolymerization, J. Am. Chem. Soc. 129 (2007) 8082–8083.

[38] F. Shi, Q. Zhang, Y. Ma, Y. He, Y. Deng, From CO oxidation to CO_2 activation: an unexpected catalytic activity of polymer-supported nanogold, J. Am. Chem. Soc. 127 (2005) 4182–4183.

[39] J. Ma, N. Sun, X. Zhang, N. Zhao, F. Xiao, W. Wei, Y. Sun, A short review of catalysis for CO_2 conversion, Catal. Today 148 (2009) 221–231.

[40] M. Tu, R.J. Davis, Cycloaddition of CO_2 to epoxides over solid base catalysts, J. Catal. 199 (2001) 85–91.

[41] G.S. Jeong, A.C. Kathalikkattil, R. Babu, Y.G. Chung, D.W. Park, Cycloaddition of CO_2 with epoxides by using an amino-acid-based Cu(II)–tryptophan MOF catalyst, Chin. J. Catal. 39 (2018) 63–70.

[42] J.F. Kurisingal, Y. Rachuri, Y. Gu, G.-H. Kim, D.-W. Park, Binary metal-organic frameworks: catalysts for the efficient solvent-free CO_2 fixation reaction via cyclic carbonates synthesis, Appl. Catal. A 571 (2019) 1–11.

[43] J. Liang, Y.-B. Huang, R. Cao, Metal–organic frameworks and porous organic polymers for sustainable fixation of carbon dioxide into cyclic carbonates, Coord. Chem. Rev. 378 (2019) 32–65.

[44] X.-Y. Li, L.-N. Ma, Y. Liu, L. Hou, Y.-Y. Wang, Z. Zhu, Honeycomb metal–organic framework with lewis acidic and basic bifunctional sites: selective adsorption and CO_2 catalytic fixation, ACS Appl. Mater. Interfaces 10 (2018) 10965–10973.

[45] Y.Z. Li, H.H. Wang, H.Y. Yang, L. Hou, Y.Y. Wang, Z. Zhu, An Uncommon Carboxyl-Decorated Metal–Organic Framework with Selective Gas Adsorption and Catalytic Conversion of CO_2, Chem.–A Eur. J. 24 (2018) 865–871.

[46] X.-F. Liu, Q.-W. Song, S. Zhang, L.-N. He, Hydrogen bonding-inspired organocatalysts for CO_2 fixation with epoxides to cyclic carbonates, Catal. Today 263 (2016) 69–74.

[47] C. Stoe, X–AREA: Program For the Acquisition and Analysis of data, Version 1.30, Stoe & Cie GmbH: Darmatadt, Germany, 2005.

[48] C. Stoe, X–RED: Program For Data Reduction and Absorption correction, Version 1.28 b,, Stoe & Cie GmbH: Darmatadt, Germany, 2005.

[49] C. StoeGermany, X–SHAPE: Program For Crystal Optimization For Numerical Absorption correction, Version 2.05, Stoe & Cie GmbH: Darmatadt, 2005.

[50] G. Sheldrick, in: SHELXL-97, Program For Crystal Structure Solution, University of Göttingen, Germany, 1997, p. 36.

[51] G. Sheldrick, SHELXL-97, Program for Crystal Structure Refinement, University of Göttingen, Göttingen, Germany, 1997.

[52] International Tables for X-ray Crystallography, Vol C, Kluwer Academic Publisher, Doordrecht, The Netherlands,1995.

[53] Stoe & CieCrystallographic Package, Version 1.07b X-STEP32, Stoe & Cie GmbH, Darmstadt, Germany, 2000.

[54] Y.A. Rulev, Z.T. Gugkaeva, A.V. Lokutova, V.I. Maleev, A.S. Peregudov, X. Wu, M. North, Y.N. Belokon, Carbocation/polyol systems as efficient organic catalysts for the preparation of cyclic carbonates, ChemSusChem 10 (2017) 1152–1159.

[55] X. Wu, C. Chen, Z. Guo, M. North, A.C. Whitwood, Metal-and halide-free catalyst for the synthesis of cyclic carbonates from epoxides and carbon dioxide, ACS Catal. 9 (2019) 1895–1906.

[56] Q.-Y. Liu, Z.-J. Xiahou, Y.-L. Wang, L.-Q. Li, L.-L. Chen, Y. Fu, 3D metal–organic frameworks constructed of 2D metal aromatic sulfonate–carboxylate layers and 1,3-di(4-pyridyl) propane pillars: syntheses, structural topologies, and luminescent properties,, CrystEngComm 15 (2013) 4930–4936.

[57] Z.-J. Xiahou, Y.-L. Wang, Q.-Y. Liu, L.-Q. Li, L.-J. Zhou, Synthesis, structure, and magnetism of a ytterbium coordination polymer with 5-sulfonyl-1,2,4-benzenetricarboxylate and oxalate, J. Coord. Chem. 66 (2013) 2910–2918.

[58] a) D. Connor, H. Krummel, Detergent composition containing a polyfunctionally-substituted aromatic acid sequestering agent, 1974; b) D. Connor, H. Krummel, Phenolic calcium-complexing agents for detergents, 1972 Google Patents, DE 1971-2164872.

[59] A.R. Hajipour, B.B.F. Mirjalili, A. Zarei, L. Khazdooz, A. Ruoho, A novel method for sulfonation of aromatic rings with silica sulfuric acid, Tetrahedron Lett. 45 (2004) 6607–6609.

[60] A.R. Moosavi-Zare, M.A. Zolfigol, E. Noroozizadeh, Regioselective sulfonation of aromatic compounds over 1,3-disulfonic acid imidazolium chloride under aqueous media, Synlett 27 (2016) 1682–1684.

[61] W.-L. Xiong, Y.-L. Wang, Q.-Y. Liu, A three-dimensional polymeric potassium complex of 5-sulfonobenzene-1, 2, 4-tricarboxylic acid: poly[μ-*aqua*-aqua-μ_9-(2,4-dicarboxy-5-sulfonatobenzoato)-dipotassium(I)], Acta Crystallogr. Sec. C 69 (2013) 1132–1135.

[62] M. Nadeem, M.H. Bhatti, U. Yunus, M. Mehmood, H.M. Asif, S. Mehboob, U. Flörke, Synthesis and characterization of unique new lithium, sodium and potassium coordination polymers, Inorganica. Chim. Acta 479 (2018) 179–188.

[63] M.G. Goesten, J. Juan-Alcañiz, E.V. Ramos-Fernandez, K.S.S. Gupta, E. Stavitski, H. van Bekkum, J. Gascon, F. Kapteijn, Sulfation of metal–organic frameworks: opportunities for acid catalysis and proton conductivity, J. Catal. 281 (2011) 177–187.

[64] Y. Zang, J. Shi, F. Zhang, Y. Zhong, W. Zhu, Sulfonic acid-functionalized MIL-101 as a highly recyclable catalyst for esterification, Catal. Sci. Technol. 3 (2013) 2044–2049.

[65] J. Chen, Z. Zhang, Z. Bao, Y. Su, H. Xing, Q. Yang, Q. Ren, Functionalized metal–organic framework as a biomimetic heterogeneous catalyst for transfer hydrogenation of imines, ACS Appl. Mater. Interfaces 9 (2017) 9772–9777.

[66] T. Takahashi, T. Watahiki, S. Kitazume, H. Yasuda, T. Sakakura, Synergistic hybrid catalyst for cyclic carbonate synthesis: remarkable acceleration caused by immobilization of homogeneous catalyst on silica, Chem. Commun. (2006) 1664–1666.

[67] F. Wall, W. Claussen, Infrared absorption studies of some glycols and ethoxyalcohols, J. Am. Chem. Soc. 61 (1939) 2679–2683.

[68] J.-W. Huang, M. Shi, Chemical fixation of carbon dioxide by NaI/PPh_3/PhOH, J. Org. Chem. 68 (2003) 6705–6709.

[69] S. Liang, H. Liu, T. Jiang, J. Song, G. Yang, B. Han, Highly efficient synthesis of cyclic carbonates from CO_2 and epoxides over cellulose/K.I, Chem. Commun. 47 (2011) 2131–2133.

[70] S. Hwang, Y.M. Byun, J.Y. Ryu, U. Farwa, H. Begum, J. Lee, S. Lee, H.-R. Park, J. Lee, Potassium coordination polymer complex containing tetrazolyl ligand, J. Mol. Struct. 1185 (2019) 50–56.

[71] J. Sun, L. Han, W. Cheng, J. Wang, X. Zhang, S. Zhang, Efficient acid–base bifunctional catalysts for the fixation of CO_2 with epoxides under metal-and solvent-free conditions, ChemSusChem 4 (2011) 502–507.

[72] Y. Zhang, S. Yin, S. Luo, C.T. Au, Cycloaddition of CO_2 to epoxides catalyzed by carboxyl-functionalized imidazolium-based ionic liquid grafted onto cross-linked polymer, Ind. Eng. Chem. Res. 51 (2012) 3951–3957.

[73] R. Arunachalam, E. Chinnaraja, A. Valkonen, K. Rissanen, P.S. Subramanian, Bifunctional coordination polymers as efficient catalysts for carbon dioxide conversion, Appl. Organomet. Chem. 33 (2019) e5202.

[74] A. Kundu, G.C. De, S. Ghosh, Green synthesis of novel polyesterurethane materials from epoxides and carbon dioxide by new set of one-dimensional coordination polymer catalyst, ACS omega 4 (2019) 14074–14084.